Australasian Transport Research Forum 2022 Proceedings
28-30 September, Adelaide, Australia
Publication website: http://www.atrf.info

A cooperative eco-driving system for mixed traffic on urban roads

Zhiwei Yang[1], Zuduo Zheng[1], Jiwon Kim[1], Hesham Rakha[2]

[1] School of Civil Engineering, University of Queensland

[2] The Charles E. Via, Jr. Department of Civil & Environmental Engineering, Virginia Tech

Email for correspondence: zhiwei.yang@uqconnect.edu.au

Abstract

Connected and automated vehicles (CAVs) provide unprecedented opportunities for optimising and precisely controlling vehicle motion to improve vehicle safety, efficiency, fuel consumption and emissions as well as ride comfort, based on the information obtained through various sensors and vehicle to everything (V2X) communication. In this paper, we establish an eco-driving system that dynamically assists CAVs traverse signalised intersections in mixed traffic including CAVs and human-driven vehicles (HVs). This eco-driving system is able to deal with uncertainty, such as cut-in HVs and prediction deviation. Specifically, an algorithm to determine the earliest arrival time at the stop line considering the effects of queue, signal phase and timing (SPaT) and vehicle's kinematic limits is developed. As for the trajectory models, The trigonometric speed model and triangular acceleration model are employed to achieve a smooth change in acceleration. Trajectory planning is realised by optimisation, and dynamically updated to cope with uncertainty. To evaluate the performance of the proposed models in both uncongested and congested traffic, microscopic simulations are conducted in a comprehensive simulation platform, SimCCAD that combines a traffic simulator (SUMO) and a robot simulator (Webots) for CAV emulation. Results show that the proposed methods significantly improve the average travel time and fuel efficiency of the subject CAV and the following HVs in uncongested traffic with safety guaranteed, and the trigonometric speed model slightly outperforms the triangular acceleration model. In congested traffic, as other researchers have found, the performance of eco-driving strategies is found to not improve travel time efficiency, however, they enhance energy saving and safety significantly.

1. Introduction

Safety, time efficiency, energy efficiency and ride comfort are important performance indicators of road transport systems. Early studies generally focused on safety and traffic efficiency. Recently, thanks to the emergence of connected and automated vehicles (CAVs), researchers gradually turn their attention to eco-driving strategies that aim to minimise energy consumption and emissions without harming safety or efficiency, by utilising information acquired via vehicle to everything (V2X) communication. Generally, eco-driving technology provides advisory speed to help drivers/CAVs avoid abrupt speed change and unnecessary kinetic energy loss.

Existing eco-driving studies either focus on freeways or urban streets. Traffic stream on freeways is rarely disturbed except at merging and diverging area. However, traffic is often interrupted by signal control at signalised intersections or by giving way to other road users at

non-signalised intersections. These interuptions often force vehicles to brake sharply, keep idling , or accelerate, which are associated with high energy consumption and emissions. Intuitively, urban intersections have higher potential and more pressing needs for improvement. Therefore, this paper focuses on eco-driving strategies for signalised urban roads.

Green Light Optimal Speed Advisory (GLOSA) system, an eco-driving technology near signalised intersections, has been developed to improve time and energy efficiency. It provides advisory speeds based on the signal phase and timing (SPaT) information with the objective of minimising idling due to red signals. Early eco-driving methods near signalised intersections predict whether the vehicle is able to travel through the intersection (Li et al., 2009), and provide an advisory target speed (Seredynski et al., 2013) or speed profiles (Mandava et al., 2009, Barth et al., 2011, Rakha and Kamalanathsharma, 2011). However, these methods unrealistically assumed that there was no queue or overtaking vehicles, thus are only applicable in uncongested traffic and cannot cope with the disturbances from surrounding vehicles. If these methods are applied in general traffic, drivers would have to either stick to the original advice even when uncertainty happens, which obviously is quite dangerous, or switch between the original advice and safe car-following mode frequently, which can cause more fluctuated speeds and ultimately harm road safety, deteriorate time and energy efficiency. Some subsequent research further considered queue (Xia et al., 2013, Yang et al., 2016, He et al., 2015, Huang et al., 2018). However, these methods are highly dependent on information from sensors, 100% CAV environment, or historical data, and the prediction is not accurate enough.

Trajectory geometric models are developed to provide advisory speed profile, which describes a desired vehicle motion with certain goals. Different trajectory geometric models have been developed to replicate equipped vehicles' behavior approaching to and departing from intersections, including constant speed (Tang et al., 2018), constant acceleration (Mandava et al., 2009), linearly decreased acceleration with speed (Chen et al., 2014), constant-throttle acceleration (Rakha and Kamalanathsharma, 2011), trigonometric speed (Barth et al., 2011), parabolic trajectory (Ghiasi et al., 2019), etc. Among them, the trigonometric speed model (Barth et al., 2011) can generate speed profile with continuous and comfort acceleration changes. In comparison, the models in Rakha et al. (2004) and Chen et al. (2014) caputre the feature that human-driven vehicles (HVs) tend to accelerate more sharply at lower speeds, whereas abrupt acceleration change (infinite jerk) exist at the start of acceleration. Despite that these models can mimic the acceleration behaviour of HVs, the consideration of comfort is inadequate. Since CAVs have the potential to avoid the discomfort commonly existing in human driving by following a smooth acceleration curve, it is not necessary to persist in a vehicle dynamics model for emulating traditional vehicles.

By reviewing the literature about eco-driving, several gaps are identified. First, all the existing trajectory geometric models except for the trigonometric speed model (Barth et al., 2011) have infinite jerk, which leads to poor ride comfort. Second, how queue is considered is either too simplistic (e.g., dependent on certain sensors or historical data) or unrealistic (e.g., assuming 100% CAV environment). In addition, most studies proved that their speed advisory system was effective in uncongested traffic, while a few researchers found the eco-driving methods had negative impacts in congested traffic (Morello et al., 2016). Moreover, the majority of the previous studies ignored uncertainty. Stop-and-go oscillations, HVs overtaking and prediction deviation are common factors that cause uncertainty, as the spatial and temporal information of shockwaves as well as the intentions of unconnected HVs are hard to be predicted precisely. Coping with such uncertainty requires dynamic prediction and updating of advisory trajectory (Kamalanathsharma and Rakha, 2014).

To bridge the above gaps, this study proposes an eco-driving system with strategies for queue prediction, trajectory planning and updating. Four methods are proposed: decentralised and partially centralised optimal control of trigonometric and triangular trajectory model (trigonometricDOC, trigonometricPCOC, triangularDOC and triangularPCOC), tested in different traffic scenarios (uncongested and congested traffic without and with a cut-in HV), and benchmarked against a popular car following (CF) model - the Intelligent Driver Model (IDM) (Treiber et al., 2000) and a baseline method from three aspects: safety, traffic efficiency and fuel consumption. The performance measures used in the benchmarking include speed profile, time-to-collision, travel time and fuel consumption. The main contribution of the study includes: 1) a new trajectory geometric model without infinite jerk is proposed; and 2) a complete eco-driving system adapted for uncertainty is proposed without strong assumptions.

The remainder of this paper is organised as follows: Section 2 illustrates the overall framework of the proposed eco-driving system. Section 3 introduces the methodologies used in the eco-driving strategies, simulation settings, platform and scenarios. Section 4 presents the results and discussions. Finally, Section 5 summarises the conclusions.

2. Framework overview

Figure 1: Schematic of the signalised intersection with the eco-driving system

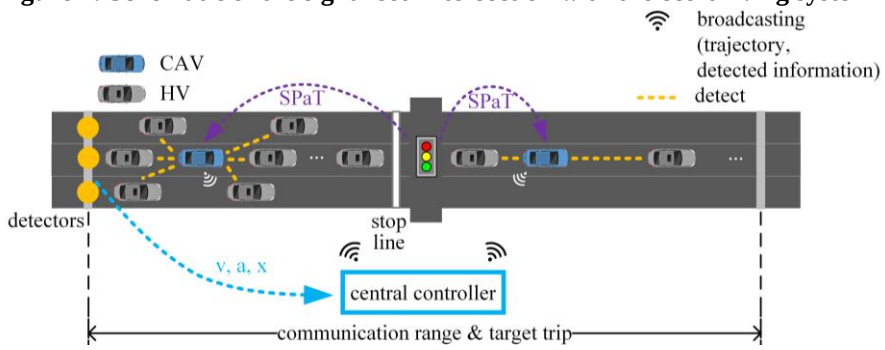

This section elaborates the traffic environment settings and operation procedures of the proposed eco-driving system. The proposed eco-driving system includes the strategies to provide advisory longitudinal speed profile without lane-changing planning, whereas HVs are allowed to change lanes. The layout of the target intersection is shown in Figure 1. Figure 2 displays the operational process of the system. To begin with, the detectors at the starting point of the communication range measure the passing vehicle's velocity, acceleration, passing location and time, which are then transmitted to the central controller. If the passing vehicle is a HV, the future trajectory will be predicted by the central controller using the IDM model based on the measured traffic states on the entry and the predicted trajectory of the preceding vehicle. If there is no preceding vehicle, the stop line is treated as a standstill preceding vehicle if the traffic signal is not green, otherwise the HV will be predicted to gradually reach the speed limit with the maximum acceleration. Then the predicted trajectory of the HV is broadcasted to CAVs in the communication zone and saved in the central controller database for queue prediction. If the passing vehicle is a CAV, the CAV starts to receive the broadcasted SPaT information, the predicted trajectories of the preceding vehicles, the planned trajectory and detected information from the other CAVs, and continues detecting the surrounding vehicles' traffic states. Based on such information, the earliest arrival time at the stop line or the end of queue is determined by considering the queue, vehicle limits and SPaT. After that, the arrival time is substituted into the trajectory model (trigonometric speed or triangular acceleration model), such that the only unknowns are the parameters representing changing rates of acceleration, which are then optimised. Afterwards, the optimised advisory trajectory is

executed unless: 1) it is not safe to implement the advisory trajectory and the IDM speed is lower than the advisory speed; or 2) the critical point with the minimum distance to the preceding vehicle when the two consecutive vehicles have the same speed has been reached and IDM speed is higher than the advisory speed. In these exceptions, IDM speed is implemented. Uncertainty from cut-in HVs or significant prediction error, is continuously monitored during the implementation. If uncertainty is detected, trajectory of the preceding vehicle will be predicted again using the newly detected data, based on which the earliest arrival time and advisory trajectory will be re-calculated. Then, the updated advisory trajectory will be implemented and the cycle repeats.

Figure 2: Operational process of the eco-driving system

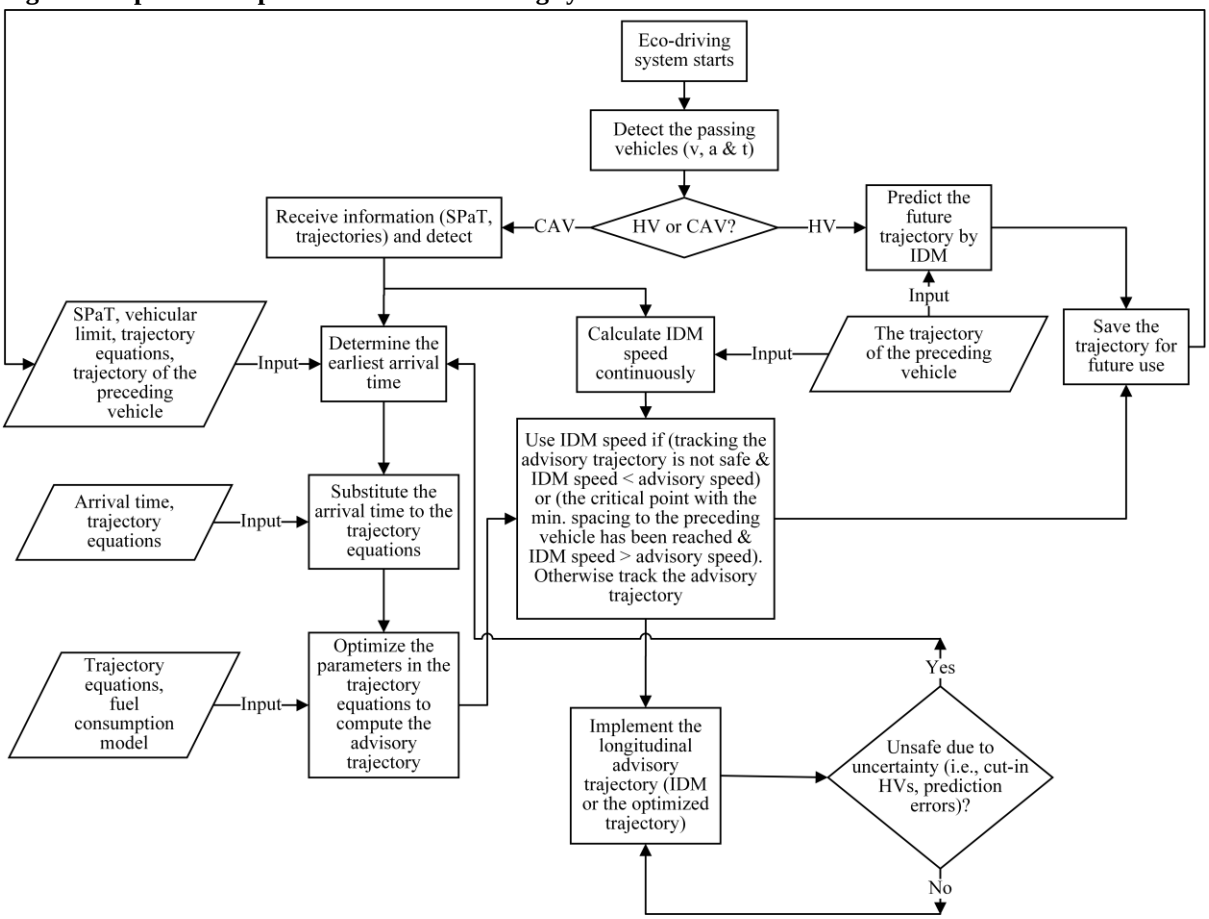

3. Methodology

This section introduces the methods used in this study. The longitudinal eco-driving strategies are elaborated in Section 3.1. The simulation platform and data are described in Section 3.2.

3.1. Longitudinal eco-driving strategies

This subsection describes the longitudinal eco-driving strategies for traversing signalised intersections, including arrival time determination in Section 3.1.1, two trajectory geometric models, i.e., trigonometric speed model and triangular acceleration model in Section 3.1.2 and 3.1.3, respectively, and trajectory optimization in Section 3.1.4.

3.1.1. Arrival time determination

When a vehicle is passing a signalised intersection, there are three factors influencing the earliest arrival time at the stop line without stopping or moving at extremely low speed, i.e., SPaT, vehicle limits (velocity, acceleration and jerk limits) and queue. Arrival time ranges

(ATRs) confined by SPaT, vehicle limits and queue, are denoted as Γ_{SPaT}, Γ_{limit} and Γ_q, respectively. The pseudocode of the algorithm for the earliest arrival time is shown below.

inputs: Information of the subject CAV on the entry: the entering time t_i, speed v_i, acceleration a_i, distance to the stop line d_{stop}; SPaT information: the start time of green light t_g and red light t_r, the start time of the next green $t_{g_next}$and the next red t_{r_next}; Information from the predicted trajectory of the preceding vehicle: the time when the preceding vehicle passes the stop line t_{pass_p}, the dissipation time of the preceding vehicle t_{diss_p} when it accelerate to v_{min}, and the corresponding speeds v_{pass_p} and v_{diss_p}, the launch time of the preceding vehicle t_{launch_p} when it can start moving, the time when the preceding vehicle accelerates to the specific speed ($v_{specific}$) $t_{specific\_p}$; The earliest and latest arrival time refined by vehicle limits and trajectory geometric model: t_e and t_l; Safety criterion: the critical time headway H_{crit}, the critical time-to-collision TTC_{crit}, the minimum speed desired for fuel efficiency v_{min}, the speed limit v_{max}.

outputs: ATRs, the earliest arrival time at the stop line for non-stop scenarios t_{arr}, arrival time at the queue end for stop scenario t_{arr}', launch time when the CAV can start moving.

for *all CAVs in communication range* **do**

$$\Gamma_{SPaT} = \begin{cases} [t_i, t_r) \cup [t_{g\_next}, t_{r\_next}], if\ green\ at\ t_i \\ [t_g, t_r], if\ yellow\ or\ red\ at\ t_i \end{cases}$$

$$\Gamma_q = \left[\max\left(t_{pass\_p}, t_{diss\_p}\right) + max(H_{crit}, TTC_{crit}), +\infty\right]$$

$\Gamma_{limit} = [t_e, t_l]$, t_e and t_l are calculated based on Equation (3), (4), (7) and (8)

if $\Gamma_{SPaT} \cap \Gamma_{limit} \cap \Gamma_q \neq \emptyset$

$t_{arr} = min\ (\Gamma_{SPaT} \cap \Gamma_{limit} \cap \Gamma_q)$

if $v_i \geq v_{min}$

$v_{avg} = d_{arr}/(t_{arr} - t_0)$

$$v_{specific} = \begin{cases} \frac{2}{3}v_{max}, if\ v_{avg} < v_{t_0} \\ v_{t_0}, if\ v_{avg} = v_{t_0} \\ 0.85v_{max}, if\ v_{avg} > v_{t_0} \end{cases}$$

if $max(v_{pass\_p}, v_{min}) < v_{specific}$

$\Gamma_q = [t_{specific\_p} + max(H_{crit}, TTC_{crit}), +\infty)$

if $\Gamma_{SPaT} \cap \Gamma_{limit} \cap \Gamma_q \neq \emptyset$

$t_{arr} = min\ (\Gamma_{SPaT} \cap \Gamma_{limit} \cap \Gamma_q)$

else

the CAV will stop, calculate t_{arr}'

$t_{launch} = max\left(t_{g\_next}, \left[t_{launch\_p} + \max(H_{crit}, TTC_{crit})\right]\right)$

3.1.2. Trigonometric speed trajectory

Once the earliest arrival time is determined, the advisory trajectory shape can be approximately determined by substituting the earliest arrival time into a trajectory model with only the parameters representing the changing rate of acceleration to be optimised. This study compares two trajectory models without infinite jerk. The trigonometric speed model will be introduced first, followed by the triangular acceleration model in Section 3.1.3.

The trigonometric trajectory was originally proposed by Barth et al. (2011), which generates a smooth trajectory ensuring that vehicle can arrive at a certain location in a specific duration, and later improved by several studies. This paper proposes a modified trigonometric speed model that combines the advantages in Altan et al. (2017) and Yang et al. (2021).

Figure 3 shows the acceleration, deceleration and stop scenario in the trigonometric speed model, represented by red, blue and yellow, respectively. From t_i to t_0, CAVs adjust the acceleration to 0 using the bounds of jerk. After that, for the non-stop scenarios, CAVs accelerate or decelerate until t_2 during which t_1 is a piecewise point dividing the speed changing segment into two with different parameters indicating changing rates of acceleration, denoted by m and n; from t_2 to t_{arr} it is a cruising segment. After t_{arr}, CAVs that just decelerated to the cruising state will accelerate back with a symmetric speed profile during which t_3 is a piecewise point similar to t_1 and reach the prior-deceleration speed at t_4, and then cruise with the same speed at t_0, while CAVs that just accelerated will remain the current speed. For the stop scenario, CAVs gradually stop by t'_{arr} (the time for the vehicle to stop at the end of queue) with m and n equal to each other. CAVs start moving at t_{launch}, before which from ${t_{arr}}'$ they are in a period of standstill, and execute the same symmetric acceleration. At ${t_4}'$ CAVs reach the prior-deceleration speed and then cruise . To save space, only the formulation for the deceleration scenario is demonstrated in Equation (1).

Figure 3: Trigonometric speed trajectory model

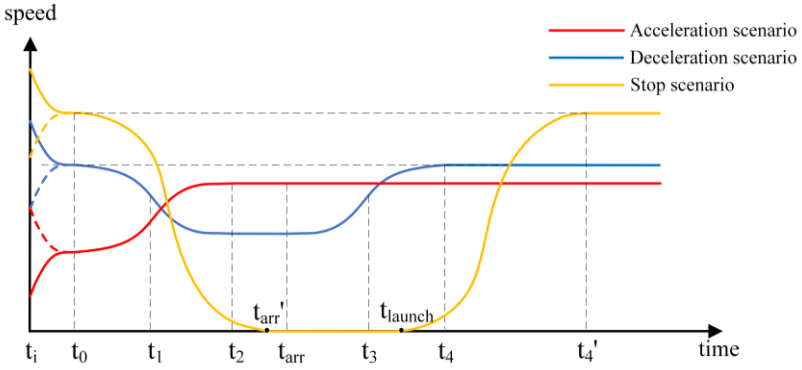

$$v_t = \begin{cases} \frac{{a_i}^2}{j_{max}} sin\left(\frac{j_{max}}{a_i}(t-t_i)\right) + v_i, t \in [t_i, t_0) \\ v_{avg} - v_{diff}\, cos[m(t-t_0)], t \in [t_0, t_1) \\ v_{avg} - v_{diff}\frac{m}{n} cos\left[n\left(t - t_2 + \frac{\pi}{n}\right)\right], t \in [t_1, t_2) \\ v_{avg} + v_{diff}\frac{m}{n}, t \in [t_2, t_{arr}) \\ v_{avg} - v_{diff}\frac{m}{n} cos\left[n\left(t - t_3 + \frac{3\pi}{2n}\right)\right], t \in [t_{arr}, t_3) \\ v_{avg} - v_{diff}\, cos[m(t-t_4)], t \in [t_3, t_4) \\ v_{t_0} = v_i + \frac{{a_i}^2}{j_{max}}, t \in [t_4, t_f] \end{cases} \quad if \begin{cases} v_{diff} < 0 \\ and \\ v_{avg} + v_{diff}\frac{m}{n} \neq 0 \end{cases} \quad (1)$$

$d_{stop} = x_{stop} - x_i$, $d_{arr} = d_{stop} - \left(\frac{\pi a_i v_i}{2j_{max}} + \frac{{a_i}^3}{{j_{max}}^2}\right)$, $\Delta t_{arr} = t_{arr} - t_0$, $v_{avg} = \frac{d_{arr}}{\Delta t_{arr}}$, $v_{diff} = v_{avg} - v_{t_0}$, $v_{t_0} = v_i + \frac{{a_i}^2}{j_{max}}$, $t_0 = t_i + \frac{\pi a_i}{2j_{max}}$, $t_1 = t_0 + \frac{\pi}{2m}$, $t_2 = t_1 + \frac{\pi}{2n}$, $t_3 = t_{arr} + \frac{\pi}{2n}$, $t_4 = t_3 + \frac{\pi}{2m}$

where a_i and v_i are the acceleration and speed at the time t_i when the CAV enters the communication range; j_{max} is the maximum jerk; v_{avg} is the advisory average speed to arrive at the stop line at the arrival time t_{arr}; v_{diff} is the difference between v_{avg} and v_{t_0}; t_f is the

final time when the CAV finishes the target trip; m and n are the parameters representing the changing rate of acceleration to be optimised; d_{stop} is the distance between the location at which the CAV has adjusted the initial acceleration to 0 and the stop line; Δt_{arr} is the duration from the time when the CAV obtains the 0 acceleration to the planned arrival time.

Constraints for jerk, acceleration, velocity and for the guarantee of obtaining a real solution are defined as:

$$\begin{gathered} a_{min} \le m v_{diff} \le a_{max} \\ j_{min} \le m^2 v_{diff} \le j_{max} \\ j_{min} \le mn v_{diff} \le j_{max} \\ v_{min} \le v_{avg} + v_{diff} m/n \le v_{max} \\ \pi/2 - 1 - n d_{arr}/v_{avg} < 0 \end{gathered} \tag{2}$$

Instead of the approximate estimations in Altan et al. (2017), the analytical solutions of the earliest and latest arrival time for the non-stop scenarios are provided here. The earliest arrival time can be calculated by solving Equation (3) and (4), whichever is larger.

$$\frac{\pi(v_{max} - v_{t_0})(v_{max} - \frac{d_{arr}}{\Delta t_{arr}})}{2a_{max}} + \frac{(v_{max} - v_{t_0})(2\frac{d_{arr}}{\Delta t_{arr}} - v_{t_0} - v_{max})}{a_{max}} - v_{max}\Delta t_{arr} + d_{arr} = 0 \tag{3}$$

$$j_{max}\Delta t_{arr}(v_{max}\Delta t_{arr} - d)(v_{max}\Delta t_{arr} - d)^2 - \left\{(v_{max} - v_{t_0})\left[\left(\frac{\pi}{2}v_{max} - v_{max} - v_{t_0}\right)\Delta t_{arr} + \left(2 - \frac{\pi}{2}\right)d\right]\right\}^2 = 0 \tag{4}$$

Similarly, the latest arrival time can be determined by replacing v_{max}, a_{max} and j_{max} with v_{min}, a_{min} and j_{min}, and then take the smaller solution from solving these two equations.

3.1.3. Triangular acceleration trajectory

To bridge the gap that most trajectory models have infinite jerk that lead to uncomfortable ride, triangular acceleration model with linear acceleration is proposed following the similar mechanism of the trigonometric speed model.

Figure 4: Triangular acceleration trajectory model

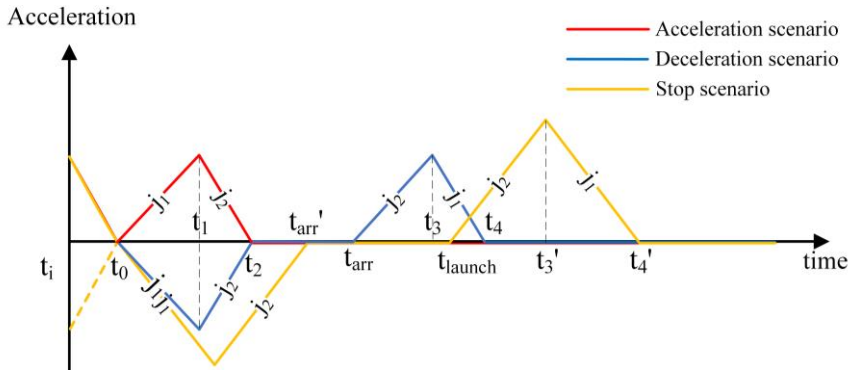

Similar to the trigonometric speed model, this model also includes the acceleration, deceleration and stop scenario, represented by the red, blue and yellow line in Figure 4, respectively. The interpretation of each stage in each scenario is the same as that of the trigonometric speed model, except that the parameters representing changing rate of acceleration are denoted as j_1 and j_2 instead of m and n, indicating the constant jerk in speed

changing segments. To save space, only the speed equations for the deceleration scenario are presented in Equation (5).

$$v_t = \begin{cases} -\frac{j_{max}}{2}(t-t_i)^2 + a_i(t-t_i) + v_i, t \in [t_i, t_0) \\ v_{t_0} + \frac{1}{2}j_1(t-t_0)^2, t \in [t_0, t_1) \\ -\frac{1}{2}j_2(t-t_1)^2 + a_{peak}(t-t_1) + v_{avg}, t \in [t_1, t_2) \\ v_{avg} + v_{diff}\frac{j_1}{j_2}, t \in [t_2, t_{arr}) \\ -\frac{1}{2}j_2(t-t_3)^2 - a_{peak}(t-t_3) + v_{avg}, t \in [t_{arr}, t_3) \\ \frac{1}{2}j_1(t-t_4)^2 + v_{t_0}, t \in [t_3, t_4) \\ v_{t_0} = v_i + \frac{{a_i}^2}{j_{max}}, t \in [t_4, t_f] \end{cases} \quad if \begin{cases} v_{diff} < 0 \\ and \\ v_{avg} + v_{diff}\frac{j_1}{j_2} \neq 0 \end{cases} \tag{5}$$

$d_{stop} = x_{stop} - x_i$, $d_{arr} = d_{stop} - \left(\frac{a_i v_i}{j_{max}} + \frac{1}{3}\frac{{a_i}^3}{{j_{max}}^2}\right)$, $\Delta t_{arr} = t_{arr} - t_0$, $v_{avg} = \frac{d_{arr}}{\Delta t_{arr}}$, $v_{diff} = v_{avg} - v_{t_0}$, $v_{t_0} = \left(v_i + \frac{{a_i}^2}{j_{max}}\right)$, $t_0 = t_i + \frac{a_i}{j_{max}}$, $a_{peak} = \pm\sqrt{2j_1 v_{diff}}$ $(same\ sign\ as\ j_1)$, $t_1 = t_0 + \frac{a_{peak}}{j_1}$, $t_2 = t_0 + \frac{a_{peak}}{j_1} + \frac{a_{peak}}{j_2} = t_1 + \frac{a_{peak}}{j_2}$, $t_3 = t_{arr} + \frac{a_{peak}}{j_2}$, $t_4 = t_3 + \frac{a_{peak}}{j_1}$

where j_1 and j_2 are the jerks at the speed changing segments to be optimised, and all the other variables have the same meaning as those in Section 3.1.2.

Constraints for jerk, acceleration and velocity are:

$$\begin{gathered} j_{min} \le j_1 \le j_{max} \\ j_{min} \le j_2 \le j_{max} \\ \sqrt{2j_1 v_{diff}} \le a_{max} \\ -\sqrt{2j_1 v_{diff}} \ge a_{min} \\ v_{min} \le v_{avg} + v_{diff} j_1 / j_2 \le v_{max} \end{gathered} \tag{6}$$

The earliest arrival time without stop considering vehicle limits can be calculated by assuming the upper limits of acceleration and velocity (a_{max} and v_{max}) or jerk and velocity (j_{max} and v_{max}) are reached, as formulated in Equation (7) and Equation (8), whichever is larger.

$$3a_{max}v_{max}{\Delta t_{arr}}^2 - [2(2v_{t_0} - v_{max})(v_{t_0} - v_{max}) + 3a_{max}d_{arr}]\Delta t_{arr} + 2d_{arr}(v_{t_0} - v_{max}) = 0 \tag{7}$$

$$9t_{arr}j_{max}(d_{arr} - v_{t_0}\Delta t_{arr})(v_{max}\Delta t_{arr} - d_{arr})^2 - 2(v_{max} - v_{t_0})^2(d - 2v_{t_0}\Delta t_{arr} + v_{max}\Delta t_{arr})^2 = 0 \tag{8}$$

Similarly, the latest arrival time can be determined by replacing v_{max}, a_{max} and j_{max} with v_{min}, a_{min} and j_{min}, and then take the smaller solution from solving these two equations.

3.1.4. Optimisation for longitudinal trajectory planning

Most papers formed a decentralised optimal control (DOC) problem to minimise the individual CAV's benefits (Almannaa et al., 2019), which has low computational load but small

improvement of the eco-driving objectives. In comparison, centralised optimal control (COC) that optimises the eco-driving objective of all the CAVs has a better performance but higher computational burden and more intensive information requirement. It is reasonable to assume that an intermediate state between DOC and COC may lead to a good trade-off. Given that CAVs are able to detect the adjacent HVs whose information can be broadcasted and received by other CAVs, partially centralised optimal control (PCOC) is developed to optimise the benefit of the CAV and the following consecutive HVs with accessible data. Considering the complexity of COC, only DOC and PCOC are implemented, which are formulated in Equation (9) and (10), respectively. Note that these terms in the two objective functions can be easily normalised, but it is not necessary in the simulation experiment presented later because the fuel consumption and travel time for this particular road segment are at a similar magnitude level.

$$DOC: Minimise \int_{t_i}^{t_f} F_t dt + t_f - t_i \tag{9}$$

$$PCOC: Minimise \int_{t_i}^{t_f} \left[\sum_{k}^{N_k} F_t\right] dt + t_f - t_i, k \in \Omega \tag{10}$$

where Ω consists of the HVs with accessible traffic states consecutively following the subject CAV; N_k is the number of HVs in Ω; k is the ordinal number; F_t is the instantaneous fuel consumption at time t; t_i and t_f are the initial time when the CAV enters and the final time when it finishes the targets trip, respectively. The decision variables are m and n if the trigonometric speed trajectory model is adopted, and j_1 and j_2 if the triangular acceleration trajectory model is adopted.

Figure 5: Illustration of spatial relationship of consecutive vehicles

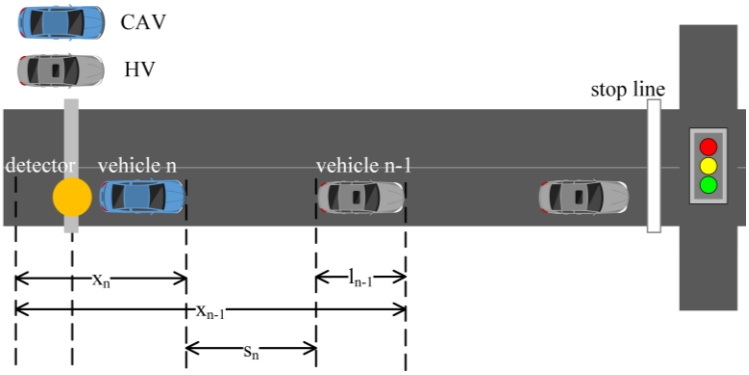

Safety issue should be checked in real time. Three factors are considered for collision avoidance: time headway (H), time-to-collision (TTC) and time displacement spacing (TDS). To ensure safety, the real time spacing should be at least larger than the minimum safe spacing calculated by the critical H and TTC (H_{crit} and TTC_{crit}), which are the minimum allowable H and TTC. TDS is defined as the spacing between the location of the vehicle at time $t + \tau_n$ and the preceding vehicle at time t, where τ_n is a pre-set time displacement during which the preceding vehicle is assumed standstill while the subject vehicle continues driving. To be more conservative, real time TDS should be larger than the minimum safe spacing calculated from H_{crit} and TTC_{crit}, as shown in Equation (11).

$$TDS_n = x_{n-1,t} - x_{n,t+\tau_n} - l_{n-1} \geq max\{S_{H_{crit},n}, S_{TTC_{crit},n}\} \tag{11}$$

$$S_{H_{crit},n} = v_n \times H_{crit} - l_{n-1} + S_s, S_{TTC_{crit},n} = (v_n - v_{n-1}) \times TTC_{crit}\ (if\ v_n > v_{n-1})$$

where $x_{n-1,t}$ is the location of vehicle $n-1$ at time t and $x_{n,t+\tau_n}$ is the location of the subject vehicle n at time $t+\tau_n$; τ_n is the pre-set time displacement; $S_{H_{crit},n}$ and $S_{TTC_{crit},n}$ represent the safe spacing between vehicle n and $n-1$ calculated from the critical H and TTC; v_n and v_{n-1} are the speed of vehicle n and $n-1$; S_s is the standstill safe spacing; l_{n-1} is the length of vehicle $n-1$. The schematic diagram of two successive vehicles is shown in Figure 5.

The Virginia Tech Comprehensive Power-based Fuel Model, Type 1 (VT-CPFM-1) is adopted to calculate instantaneous fuel consumption F_t because it is simple, accurate and easy to be calibrated using public fuel consumption data (Almannaa et al., 2019). Besides, VT-CPFM does not result in sharp engine torque or acceleration. The formulation of VT-CPFM can be found in Rakha et al. (2011). It is noteworthy that the parameters related to vehicle attributes are from the brochure of the simulated vehicle model, i.e., BMW x5, while the physical parameters are from Rakha et al. (2011).

3.2. Simulation

Figure 6: Simulation scenarios

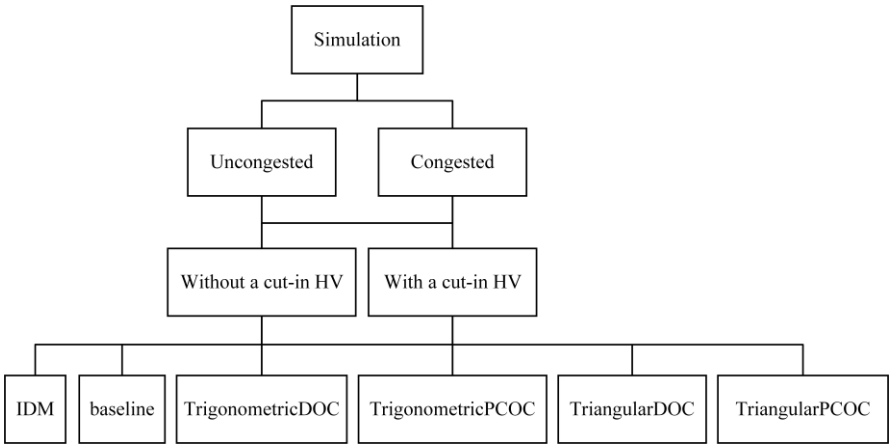

This section introduces the simulation settings, platform and scenarios in this study. To test the effectiveness of the proposed eco-driving strategies, simulations in a real intersection with assumed traffic data (SPaT, HV trajectories and CAV trajectories without using the proposed strategies) are conducted. The target intersection is from Peachtree Street & 10th Street, Atlanta, GA, because the geographic data are available from OpenStreetMap and HV trajectory data are available from the celebrated NGSIM open dataset. The simulation platform is SimCCAD, integrating SUMO and Webots, where SUMO simulates road traffic and HV driving while Webots is for accurately simulating CAVs (Jia et al., 2021). The platform is more realistic than solely using a traffic simulator thanks to the robotic modelling of CAV behaviour by Webots. For more detail on SimCCAD, see (Jia et al., 2021).

The simulation scenarios are summarised in Figure 6. The four proposed methods, i.e., trigonometricDOC, trigonometricPCOC, triangularDOC and triangularPCOC are evaluated and compared with IDM model without any eco-driving strategy and a baseline method. Although the objective function in the baseline method is the same as in DOC, the baseline method is not as good as the proposed methods, as reflected in the following four points. First, in the baseline method, the lower bound of the arrival time range confined by queue is simply a safe buffer (the maximum of the critical H and TTC) after the preceding vehicle starts moving. Second, the arrival time range constrained by vehicle limits is just an estimation following Altan et al. (2017). Third, the trajectory planning in the baseline method is static.

And finally, in the baseline method, CAVs will only switch to CF mode if the future safe spacing is not satisfied.

Two traffic conditions, uncongested and congested traffic (the CAV enters with a speed of 12.14m/s and 3.75m/s, respectively) are simulated using these six methods, where there is one CAV and all other vehicles are HVs. Two scenarios are estimated, i.e., the CAV driving without and with a cut-in HV. For each scenario in congested and uncongested traffic, ten simulations are conducted for each method (that is, 240 simulation runs in total).

4. Result analysis

The simulation results in uncongested and congested traffic are presented in Section 4.1 and 4.2. Speed profile, TTC distribution, travel time, and fuel consumption were estimated to assess the performance of each method. To save space, only the speed profiles and TTC diagrams from one simulation run using IDM, the baseline method and trigonometricDOC are presented, as the diagrams using the other three proposed methods are similar to that of trigonometricDOC method. However, the results for all six methods are summarised in Table 1 and Table 2.

4.1. Uncongested traffic

This section discusses the simulation results in uncongested traffic. Overall, for both the scenario without and with a cut-in HV in uncongested traffic, the proposed methods are superior to the two benchmark methods, especially in the case without a cut-in HV. To save space, only the results of the scenario with a cut-in HV are presented.

Figure 7: Speed profiles of the CAV with a cut-in HV in uncongested traffic using IDM, the baseline method and trigonometricDOC

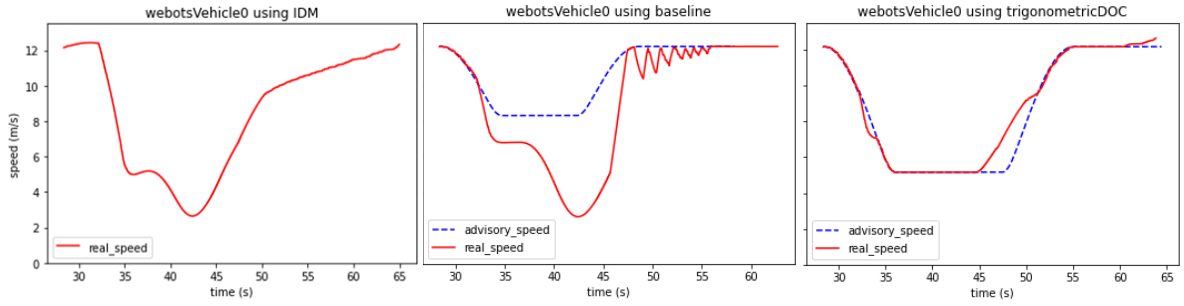

The speed profiles for the CAV with a cut-in HV in uncongested traffic are depicted in Figure 7. The IDM speed diagram including two stages of deceleration shows that the CAV was influenced by the stop-and-go oscillations generated by the red signal and the cut-in HV. For the baseline method, the advisory speed profile is abandoned for most of the trip and causes serious speed fluctuations from t=48s to t=55s due to the short spacing, cut-in vehicle and static trajectory planning. As for trigonometricDOC, compared to IDM, the eco-driving speed profile has a higher minimum speed, which not only leads to a shorter travel time, but also a smaller energy loss for speed recovery at the downstream. Compared to the baseline, although trigonometricDOC advises a lower cruising speed which seems to waste more energy, it guarantees a better advisory speed tracking by considering the acceleration time of the preceding vehicle, as reflected by the fact that the observed speed profile macthes nicely the advisory speed profile generated by trigonometricDOC for most part of the trip. Note that for trigonometricDOC, the real speed becomes larger than the advisory speed at the end of cruising part because the CAV detected that the critical point with the minimum spacing was reached and IDM speed was higher so that it switched to CF mode for time-saving.

Table 1: Percentage difference compared to IDM for the scenario with a cut-in HV in uncongested traffic

%	Baseline		trigonometric DOC		trigonometric PCOC		triangular DOC		triangular PCOC	
	travel time	total fuel	travel time	total fuel	travel time	total fuel	travel time	total fuel	travel time	total fuel
CAV	-6.26	84.71	-3.15	-2.67	-5.12	4.36	-3.21	1.30	-4.91	5.28
HV1	-5.42	-1.03	-2.63	-5.63	-4.76	-7.14	-2.67	-5.22	-4.57	-6.88
HV2	-5.07	-3.18	-2.42	-4.04	-4.56	-6.65	-2.40	-3.88	-4.36	-6.36
HV3	-4.72	-3.49	-2.29	-2.71	-4.39	-5.10	-2.30	-2.66	-4.19	-4.84
HV4	-4.49	-3.75	-2.19	-2.29	-4.23	-4.23	-2.19	-2.30	-4.02	-3.93
avg of 5	-5.20	13.86	-2.54	-3.54	-4.62	-3.90	-2.56	-2.66	-4.42	-3.50

Figure 8: TTC histograms of the CAV with a cut-in HV in uncongested traffic using IDM, the baseline method and trigonometricDOC

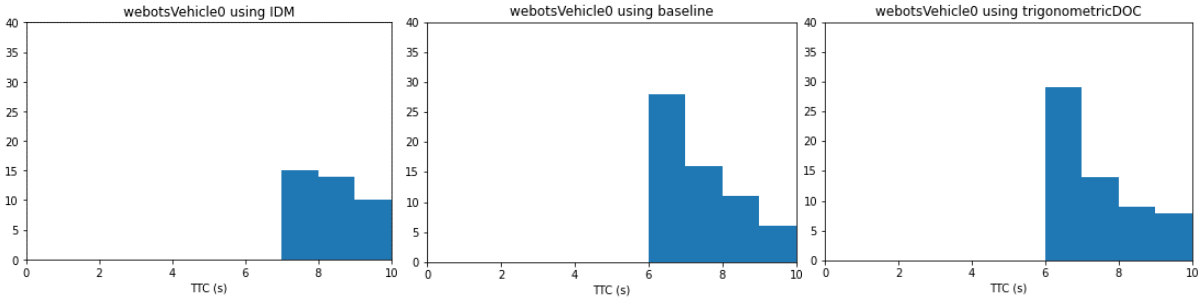

The travel time, fuel consumption of the CAV and the following HVs that passed the intersection within the same green time are calculated for each method, and the percentage differences compared to IDM are shown in Table 1. It can be seen from the results of the proposed methods that despite of the increased fuel consumption of the CAV, the travel time is reduced. In addition, both the travel time and fuel consumption of the following HVs are reduced and finally it leads to the improved average travel time and fuel consumption of all the vehicles passing the intersection in the same cycle. In comparison, the baseline method increases the fuel consumption of the CAV more significantly than the decrease in travel time, because it generates lots of speed fluctuations as a result of frequent switching between IDM and the advisory speed. As for the performance comparison among the four developed methods, for the CAV, PCOC performs much worse in fuel-saving than DOC but reduces travel time slightly more than DOC; for the following HVs, PCOC improves both fuel and travel time more than DOC. Also, the trigonometric method tends to be a bit better than the triangular method in travel time and energy saving.

To evaluate the safety performance of these methods, distribution of TTC less than 10s for each methods was analysed and compared. Figure 8 display the TTC histograms of the CAV with a cut-in HV. Compared to IDM, trigonometricDOC created incidences of TTC between 6 to 7s, which is still safe and thus acceptable. Meanwhile, the proposed methods and the baseline method have a similar safety performance.

4.2. Congested traffic

This section discusses the simulation results in congested traffic. Overall, the results indicate that the proposed methods lead to slightly worse time efficiency but much better energy efficiency than IDM, and perfom significantly better than the baseline method in all aspects.

Since the results are similar in the scenario without and with a cut-in HV, to save space, only the results of the latter scenario are presented.

Figure 9: Speed profiles of the CAV with a cut-in HVs in congested traffic using IDM, the baseline method and trigonometricDOC

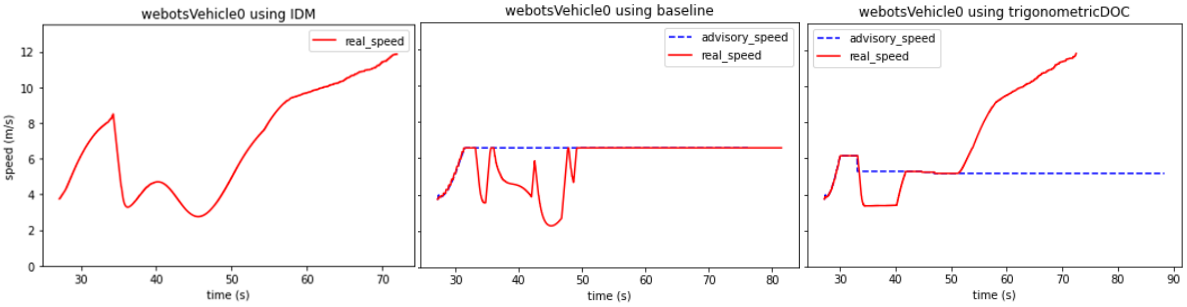

In terms of the speed profiles shown in Figure 9, those generated by the proposed methods seem a bit smoother than IDM. It can be inferred that the proposed methods may result in less fuel consumption as they advise less acceleration and deceleration. Due to the flexible switching rule between the advisory speed and IDM speed, the proposed methods allow the CAV to use the higher IDM speed when the critical point with the minimum spacing to the preceding vehicle has been reached, which results in higher time efficiency compared to the baseline method. As for the baseline, the fluctuated speed profile indicates the frequent switching between advisory speed tracking and safe car-folloing mode. It is due to the no longer applicable advisory speed profile when uncertainty occurs and that there is no updating mechanism.

Table 2: Percentage difference compared to IDM for the scenario with a cut-in HV in congested traffic

%	Baseline		trigonometric DOC		trigonometric PCOC		triangular DOC		triangular PCOC	
	travel time	total fuel	travel time	total fuel	travel time	total fuel	travel time	total fuel	travel time	total fuel
CAV	21.09	-0.31	1.24	-8.47	1.17	-2.19	1.17	-7.44	1.15	-6.66
HV1	18.25	16.61	-0.26	-0.92	-0.39	-0.03	-0.32	-0.90	-0.33	-1.02
HV2	16.61	18.68	-0.49	0.38	-0.42	0.28	-0.47	0.31	-0.40	0.24
avg of 3	18.67	11.82	0.17	-2.94	0.12	-0.63	0.14	-2.62	0.15	-2.44

The travel time, fuel consumption of the CAV and the following HVs that passed the intersection within the same green time are calculated for each method, and the percentage differences compared to IDM are shown in Table 2. It is found that the proposed methods increase the travel time of CAV by 1.15% to 1.24% but reduce the fuel consumption by 2.19% to 8.47%; increase the average travel time by 0.12% to 0.17% whereas reduce the average fuel consumption by 0.63% to 2.94%. Compared to the baseline method, the proposed methods performed much better in both travel time and fuel consumption.

To evaluate the safety performance, distribution of TTC less than 10s for each method was analysed. Figure 10 displays the TTC histograms of the CAV with a cut-in HV. It clearly shows that the proposed methods eliminate the duration with TTC less than 5s compared to IDM and the baseline method, indicating that the safety is improved by the proposed methods.

Figure 10: TTC histograms of the CAV with a cut-in HVs in congested traffic using IDM, the baseline method and trigonometricDOC

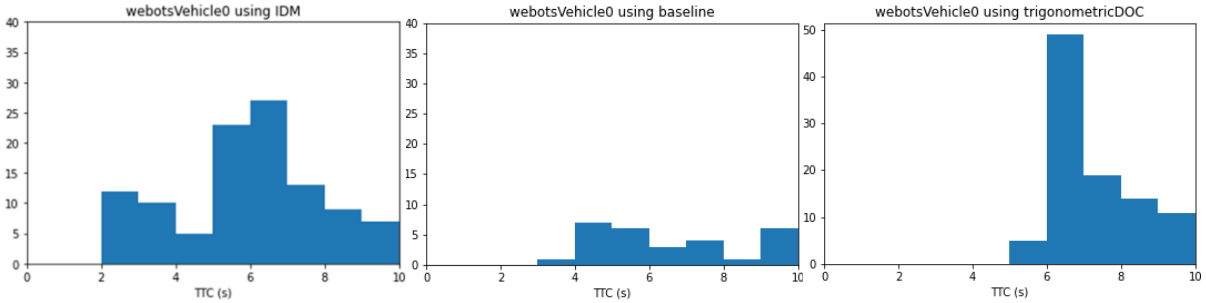

5. Conclusions

The study developed an eco-driving system for a mixed traffic near a signalised intersection, which is applicable to a general traffic with uncertainty. It is found that the eco-driving strategies are beneficial in uncongested traffic with respect to safety, efficiency, and fuel consumption. Although the proposed methods perform slightly worse than the IDM model in congested traffic regarding time efficiency, they improve safety and energy efficiency significantly. The worse time efficiency is probably due to the difficulty in predicting the preceding vehicle's behaviour accurately. Despite of the advisory speed updating mechanism, the travelled distance based on the previous plan is irretrievable. Hence, a method not dependent on the accuracy of queue prediction may be superior in dealing with the stochasticity in congested traffic.

This study is one of the first to propose an eco-driving system adapted for uncertainty without strong assumptions, , which is easier to be implemented in practice.

Acknowledgements: Financial support was received from the Australian Federal Government through the Australian Research Council (DP DP210102970) and iMOVE Australia Limited.

References

ALA, M. V., YANG, H. & RAKHA, H. 2016. Modeling evaluation of eco–cooperative adaptive cruise control in vicinity of signalized intersections. Transportation Research Record, 2559, 108-119.

ALMANNAA, M. H., CHEN, H., RAKHA, H. A., LOULIZI, A. & EL-SHAWARBY, I. 2019. Field implementation and testing of an automated eco-cooperative adaptive cruise control system in the vicinity of signalized intersections. Transportation research part D: transport and environment, 67, 244-262.

ALTAN, O. D., WU, G., BARTH, M. J., BORIBOONSOMSIN, K. & STARK, J. A. 2017. Glidepath: Eco-friendly automated approach and departure at signalized intersections. IEEE Transactions on Intelligent Vehicles, 2, 266-277.

BARTH, M., MANDAVA, S., BORIBOONSOMSIN, K. & XIA, H. Dynamic ECO-driving for arterial corridors. 2011 IEEE Forum on Integrated and Sustainable Transportation Systems, 2011. IEEE, 182-188.

CHEN, Z., ZHANG, Y., LV, J. & ZOU, Y. 2014. Model for optimization of ecodriving at signalized intersections. Transportation Research Record, 2427, 54-62.

GHIASI, A., LI, X. & MA, J. 2019. A mixed traffic speed harmonization model with connected autonomous vehicles. Transportation Research Part C: Emerging Technologies, 104, 210-233.

HE, X., LIU, H. X. & LIU, X. 2015. Optimal vehicle speed trajectory on a signalized arterial with consideration of queue. Transportation Research Part C: Emerging Technologies, 61, 106-120.
HUANG, K., YANG, X., LU, Y., MI, C. C. & KONDLAPUDI, P. 2018. Ecological driving system for connected/automated vehicles using a two-stage control hierarchy. IEEE Transactions on Intelligent Transportation Systems, 19, 2373-2384.
JIA, D., SUN, J., SHARMA, A., ZHENG, Z. & LIU, B. 2021. Integrated simulation platform for conventional, connected and automated driving: A design from cyber–physical systems perspective. Transportation Research Part C: Emerging Technologies, 124, 102984.
KAMALANATHSHARMA, R. K. & RAKHA, H. A. 2014. Agent-based simulation of ecospeed-controlled vehicles at signalized intersections. Transportation Research Record, 2427, 1-12.
LI, M., BORIBOONSOMSIN, K., WU, G., ZHANG, W.-B. & BARTH, M. 2009. Traffic energy and emission reductions at signalized intersections: a study of the benefits of advanced driver information. International Journal of Intelligent Transportation Systems Research, 7, 49-58.
MANDAVA, S., BORIBOONSOMSIN, K. & BARTH, M. Arterial velocity planning based on traffic signal information under light traffic conditions. 2009 12th International IEEE Conference on Intelligent Transportation Systems, 2009. IEEE, 1-6.
MORELLO, E., TOFFOLO, S. & MAGRA, G. 2016. Impact analysis of ecodriving behaviour using suitable simulation platform (ICT-EMISSIONS project). Transportation Research Procedia, 14, 3119-3128.
RAKHA, H. & KAMALANATHSHARMA, R. K. Eco-driving at signalized intersections using V2I communication. 2011 14th international IEEE conference on intelligent transportation systems (ITSC), 2011. IEEE, 341-346.
RAKHA, H., SNARE, M. & DION, F. 2004. Vehicle dynamics model for estimating maximum light-duty vehicle acceleration levels. Transportation Research Record, 1883, 40-49.
RAKHA, H. A., AHN, K., MORAN, K., SAERENS, B. & VAN DEN BULCK, E. 2011. Virginia tech comprehensive power-based fuel consumption model: model development and testing. Transportation Research Part D: Transport and Environment, 16, 492-503.
SEREDYNSKI, M., MAZURCZYK, W. & KHADRAOUI, D. Multi-segment green light optimal speed advisory. 2013 IEEE International Symposium on Parallel & Distributed Processing, Workshops and Phd Forum, 2013. IEEE, 459-465.
TANG, T.-Q., YI, Z.-Y., ZHANG, J., WANG, T. & LENG, J.-Q. 2018. A speed guidance strategy for multiple signalized intersections based on car-following model. Physica A: Statistical Mechanics and its Applications, 496, 399-409.
TREIBER, M., HENNECKE, A. & HELBING, D. 2000. Congested traffic states in empirical observations and microscopic simulations. Physical review E, 62, 1805.
XIA, H., WU, G., BORIBOONSOMSIN, K. & BARTH, M. J. Development and evaluation of an enhanced eco-approach traffic signal application for connected vehicles. 16th International IEEE Conference on Intelligent Transportation Systems (ITSC 2013), 2013. IEEE, 296-301.
YANG, H., RAKHA, H. & ALA, M. V. 2016. Eco-cooperative adaptive cruise control at signalized intersections considering queue effects. IEEE Transactions on Intelligent Transportation Systems, 18, 1575-1585.
YANG, Z., FENG, Y. & LIU, H. X. 2021. A cooperative driving framework for urban arterials in mixed traffic conditions. Transportation research part C: emerging technologies, 124, 102918.